Microsecond Rotational Dynamics of F-Actin in ActoS1 Filaments during ATP Hydrolysis†

Choi-man Ng and Richard D. Ludescher*

Department of Food Science, Rutgers University, and New Jersey Agricultural Experiment Station, Cook College, New Brunswick, New Jersey 08903-0231

Received March 9, 1994; Revised Manuscript Received May 23, 1994®

ABSTRACT: Rabbit skeletal muscle F-actin labeled at Cys374 with the triplet probe erythrosin-5-iodoacetamide had a steady-state phosphorescence anisotropy ($\bar{r}_p$) of 0.090 ± 0.005 at 20 °C in 100 mM KCl, pH 7.0, buffer. Titration with skeletal muscle S1 fragment increased $\bar{r}_p$ to 0.138 ± 0.006 at a mole ratio of 1:1. In the presence of ATP, the anisotropy of the actoS1 complex initially decreased to 0.050 ± 0.005, a value significantly smaller than the anisotropy of pure F-actin; $\bar{r}_p$ subsequently increased to 0.126 ± 0.002. The time course of the increase matched that expected from the measured actin-activated ATPase of S1. The plateau value at long time, 0.126, was identical to that of actoS1 in the presence of exogenous ADP or ADP plus phosphate. Characterization of the spectroscopic properties of the erythrosin probe indicated that the changes in $\bar{r}_p$ were not due to changes in fast probe motions on the surface of the filament or the phosphorescence emission lifetime, or in the orientation of the probe on the surface of F-actin, suggesting that they reflect large-scale changes in the microsecond rotational dynamics of actin. ATP hydrolysis by actoS1 thus appeared to induce rotational motions of or within F-actin on the phosphorescence time scale (≈300 μs). Although the precise physical origin of the induced rotational motions is unknown, this study provides direct evidence that large-scale conformational fluctuations of the actin filament are associated with the force-generating event in actomyosin.

Skeletal muscle is organized as a regular array of interdigitated thick, myosin-containing, and thin, actin-containing, filaments whose vectorial movement causes muscle contraction (Bagshaw, 1982). Filament sliding is driven at the molecular level by a cycle of attachment and detachment of myosin heads (crossbridges) to actin in the thin filaments; this cycle is fueled by ATP hydrolysis on the myosin head. The molecular mechanism by which this cycle is coupled to force generation is unknown. Although myosin is the motor that drives vectorial motion through hydrolysis of MgATP and release of products from the actomyosin complex, several studies suggest that structural changes within the actin filament play an important, if not essential, role in this process.

Although current thinking on the mechanism of force generation generally assigns a passive role to actin, its precise role in the molecular mechanism of force generation is actually unknown. Recent research [reviewed in Morel and Merah (1992)] suggests that conformational changes occur in F-actin during interaction with ATP-hydrolyzing myosin heads and that these changes may be associated with the molecular mechanism of force generation. Direct physical modification of the F-actin structure either by proteolysis (Schwyter et al., 1990) or by cross-linking (Prochniewicz & Yanagida, 1990; Prochniewicz et al., 1993) has been shown to decrease actin motility *in vitro* without comparable decreases in the MgATPase activity. These studies suggest that the generation of energy by myosin can be uncoupled from filament movement by modifying the structure of F-actin. A single site mutation in actin from *Drosophila melanogaster* (E316K) has also been shown to modulate the mechanical properties of flight muscle without influencing the binding of myosin to actin (Drummond et al., 1990). Cryomicroscopy studies show that there are structural changes in F-actin that are associated with binding subfragment 1 (S1)[1] (Menetret et al., 1991).

Several studies indicate that ATP hydrolysis by actomyosin directly induces structural changes in the actin filament. Yanagida et al. (1984) showed using optical microscopy that the bending fluctuations of thin filament complexes with bound HMM were dramatically increased in the presence of MgATP only when the filaments were activated with Ca^{2+}, suggesting that ATP hydrolysis by the attached heads induced active bending of the filaments. The translational diffusion coefficient of actoHMM complexes was also found to increase in the presence of MgATP during active hydrolysis (Burlacu & Borejdo, 1992).

Visual observations of filament motion in *in vitro* surface motility assays provide direct evidence for induced rotational motions within the actin filament during movement (Tanaka et al., 1992; Nishizaka et al., 1993). Force generation in the actomyosin complex apparently imparts a right-handed twisting motion to the F-actin filament (Nishizaka et al., 1993), indicating that the force-generating event imparts a torque to F-actin. The possible functional significance of this induced rotational motion is as yet unknown.

An atomic model of F-actin has been generated (Holmes et al., 1990) from the structure of actin–DNase I (Kabsch et al., 1990). This model has been combined with the atomic

† This work was supported by grants-in-aid from the Muscular Dystrophy Association and the American Heart Association—New Jersey Affiliate, and by funds provided by the State of New Jersey. This is Publication No. D-10567-2-94 of the New Jersey Agricultural Experiment Station.

* Address correspondence to this author at the Department of Food Science, Rutgers University.

® Abstract published in *Advance ACS Abstracts,* July 1, 1994.

[1] Abbreviations: actoS1, complex of F-actin with subfragment 1; DTT, dithiothreitol; EDTA, ethylenediaminetetraacetic acid; EPPS, *N*-(2-hydroxyethyl)piperazine-*N*′-3-propanesulfonic acid; FWHM, full width at half-maximum; HMM, heavy meromysin; LMM, light meromysin; MOPS, 4-morpholinepropanesulfonic acid; P_i, phosphate; PMSF, phenylmethanesulfonyl fluoride; SDS, sodium dodecyl sulfate; S1, subfragment 1.

0006-2960/94/0433-9098$04.50/0

structure of the myosin head (S1) (Rayment et al., 1993a) to generate a model for the actomyosin complex (Rayment et al., 1993b) and to propose molecular mechanisms for force generation.

Studies of the molecular mechanism of force generation and its regulation are thus favorably positioned. A detailed mechanism, however, must also be based on dynamic studies of conformational changes occurring within the myosin/thin filament complex during activation and force generation. The rotational dynamic studies reported here attempt to animate the molecular models with direct measurements of the large-scale conformational dynamics that occur in the thin filament during force generation.

We have used steady-state phosphorescence anisotropy from the triplet probe erythrosin-5-iodoacetamide covalently attached to Cys374 of actin (Ludescher & Liu, 1993) to monitor the large-scale rotational dynamics of F-actin during interaction with myosin heads (S1). In the rigor complex of S1 bound to F-actin (actoS1), the actin filaments were found to be nearly immobile on the microsecond time scale. Upon addition of MgATP to this complex, the rotational motions of the filaments increased; the rotational dynamics of actoS1 during ATP hydrolysis were more extensive than the dynamics of pure actin filaments. ATP hydrolysis by actoS1 thus appeared to induce rotational motions of or within F-actin on the phosphorescence time scale (≈300 μs). Although the precise physical origin of the induced rotational motions is unknown, this study provides direct evidence that large-scale conformational fluctuations of the actin filament are associated with the force-generating event in actomyosin.

MATERIALS AND METHODS

Protein Preparations and Labeling. Actin was isolated from the skeletal muscle of New Zealand white rabbits. Acetone powder was prepared from the leg and back muscles according to standard protocols (Pardee & Spudich, 1982) and stored in a sealed bottle at −20 °C. Actin was extracted from acetone powder into G-buffer (1 mM EPPS, 0.2 mM $CaCl_2$, 1 mM NaN_3, and 0.2 mM ATP, pH 8.5) containing 0.5 mM DTT and purified using the procedures of Thomas et al. (1979). Actin was stored as filaments by dialysis against F-buffer (10 mM MOPS, 100 mM KCl, 2 mM $MgCl_2$, 0.2 mM $CaCl_2$, 1 mM NaN_3, and 0.2 mM ATP, pH 7.0) at 0 °C as described elsewhere (Ludescher & Liu, 1993). Actin concentration was determined by the absorbance at 290 nm using an extinction coefficient of 0.63 $(mg/mL)^{-1}$ cm^{-1} for actin. Actin was labeled with erythrosin-5-iodoacetamide (Molecular Probes, Inc., Eugene, OR) using a modification of the procedure of Sawyer et al. (1988); typical preparations had a dye:protein ratio of about 0.8. Actin preparation, labeling, and characterization protocols are described in detail in Ludescher and Liu (1993).

Myosin was also extracted from the skeletal muscle of New Zealand white rabbits. Myofibrils were prepared from minced leg and back muscles as described in Thomas et al. (1980), and myosin was purified from myofibrils as described in Eads et al. (1984). The purified myosin was stored at −20 °C in myosin buffer (0.5 M KCl, 0.5 mM EDTA, 0.5 mM DTT, and 20 mM MOPS, pH 7.0) containing 50% glycerol (v/v) as an antifreeze. Subfragment 1 (S1) was prepared from myosin after proteolysis in the presence of 0.05 mg/mL α-chymotrypsin (Sigma Chemical Co., St. Louis, MO) with gentle stirring in a 25 °C water bath according to the method of Weeds and Taylor (1975); the digestion was terminated by adding 1/100 volume of 0.1 M PMSF. S1 was stored by dialysis at 0 °C against S1 buffer (30 mM KCl, 10 mM MOPS, and 1 mM EDTA, pH 7.0) containing 0.5 mM DTT and 1 mM NaN_3. In order to ensure the stability of S1, samples were used within 1 week of preparation.

Biochemical Procedures. The purity of samples was checked by SDS–polyacrylamide gel electrophoresis (Eads et al., 1984). The MgATPase activity of S1 was determined in the absence or presence of F-actin by measuring the release of inorganic phosphate after ATP hydrolysis in FB′ buffer (FB′: 30 mM KCl, 0.1 mM DTT, 2 mM $MgCl_2$, 0.2 mM $CaCl_2$, 1 mM NaN_3, 10 mM MOPS, and 0.2 mM ATP, pH 7.0). The reaction was initiated by the addition of ATP and terminated by the addition of 4% sodium citrate. Phosphate was determined colorimetrically using the malachite green method. At least three assay tubes with different incubation times (1, 2, and 4 min) were used for each measurement; the absorbance at 660 nm was monitored for each tube. Plots of A_{660} versus incubation time (minutes) were fit by linear regression analysis; the slope of this line is related to the ATPase activity:

$$\text{slope} = (\text{IU})A_{(660)\text{std}}[\text{S1}]_{\text{assayed}}/[\text{P}_\text{i}]_{\text{std}}$$

where IU = activity = micromoles of P_i generated per milligram of S1 assayed per minute, $A_{(660)\text{std}}$ is the absorbance of a phosphate standard, and $[P_i]_{std}$ is the concentration of the phosphate standard (typically 0.4 mM).

The activity was also used to calculate the time (t) for hydrolysis of ATP as a function of the concentration of S1 at 20 °C using the equation:

$$t = ([\text{ATP}]/\text{IU})/[\text{S1}]$$

where the time t is in minutes, [ATP] is expressed in millimolar, and [S1] is expressed in milligrams per milliliter.

Spectroscopic Measurements. Steady-state fluorescence measurements were made on a SPEX Model F1T11 spectrofluorometer (SPEX Industries, Metuchen, NJ) equipped with a 450-W high-pressure xenon lamp, single-grating excitation and emission monochromators, dual emission monochromators in a T-format, Glan–Thompson crystal polarizers on excitation and emission, and a circulating water bath to control the temperature of the sample. This instrument was under the control of a microcomputer running DM3000F software (SPEX Industries). Samples for spectroscopic measurements were prepared by mixing labeled actin with unlabeled actin to adjust the total concentration of erythrosin to 1.0 μM and the total concentration of actin (labeled + unlabeled) to 12 μM (0.5 mg/mL). This gave a final dye: protein ratio of about 0.08 and a maximum absorbance at the peak of the erythrosin absorption of about 0.06. All luminescence measurements were done under anaerobic conditions using an enzymatic deoxygenation system (Horie & Vanderkooi, 1981).

Steady-state fluorescence emission anisotropy spectra with 3.8 nm bandwidth resolution were collected with excitation at 500 nm (7.6 nm bandwidth). Samples were excited with both vertically and horizontally polarized light, and the fluorescence emission was collected with polarization vertical (v) and horizontal (h). This gave the four polarized intensities I_{vv}, I_{vh}, I_{hv}, and I_{hh}. Fluorescence emission anisotropy was calculated as

$$\bar{r} = (R - 1)/(R + 2)$$

where $R = (I_{vv}/I_{vh})(I_{hh}/I_{hv})$. This procedure adjusted the polarization intensity values for the differential instrument

detection efficiency of horizontal and vertically polarized emission as a function of wavelength.

Phosphorescence steady-state anisotropy and emission intensity decay measurements were made on the SPEX fluorometer equipped with a Model 1934D phosphorimeter attachment that included a low-pressure, 10-W, pulsed Xe lamp and a gated delay amplifier. The phosphorescence emission anisotropy was collected at 680 nm with excitation at 500 nm, using a time delay of 0.07 ms after flash and a total sample window of 1.5 ms. Intensities of all four polarizations were collected as above and used to calculated the anisotropy. Phosphorescence emission decays were collected without polarization and used an initial time delay of 0.07 ms, and a total decay window of 1.5 ms; the intensity was collected every 0.01 ms, and a time window of 0.01 ms was used at each time point. The decays were fit to exponential decay models using a nonlinear least-squares iterative analysis program (NFIT, Island Products, Galveston, TX). The goodness of fit was evaluated by examination of the residuals (data–fit) and the fit χ^2 values. Good fits had residuals randomly distributed about 0 and χ^2 values in the range 1–1.4. Since our previous study (Ludescher & Liu, 1993) found that a single-exponential decay provided an adequate fit to the intensity decays of erythrosin-labeled F-actin collected on our instrument, we report here single-exponential fits to the decay data that provide an adequate measure of the average lifetime of the probe.

Interpretation of Steady-State Anisotropy. The interpretation of the steady-state anisotropy in terms of specific molecular properties presents some difficulties due to the inherent ambiguity of the measurement. We can illustrate this by comparison of the expressions for the steady-state anisotropy calculated from two different models for the rotational motion of a long filament: rotation about the long axis of a rigid rod or torsional rotation about the long axis of a flexible rod.

If the anisotropy depolarizes due to the rotational diffusion about the long axis of a rigid rod, the time-resolved anisotropy [$r(t)$] decays according to the general function (Cherry, 1985; Brand et al., 1985):

$$r(t) = r_0\{\alpha_1 \exp(-t/\phi) + \alpha_2 \exp(-t/4\phi) + \alpha_3\} \quad (1)$$

where r_0 is the initial value of the anisotropy at time zero, the α_i terms are direction sines and cosines for the orientation of the emission dipole with respect to the long filament axis [see Ludescher and Ludescher (1993) for explicit expressions], and ϕ is the rotational correlation time for rotational diffusion about the long molecular axis. The steady-state anisotropy of a chromophore that depolarizes according to this expression (assuming a single lifetime τ) is

$$\bar{r}_{diff} = r_0\{\alpha_1/(1 + \tau/\phi) + \alpha_2/(1 + \tau/4\phi) + \alpha_3\} \quad (2)$$

For the phosphorescence emission anisotropy, r_0 is not the intrinsic anisotropy of the triplet–singlet transition but the value of the anisotropy remaining after any fast chromophore motions are complete (Wahl et al., 1970; Ludescher & Liu, 1993).

If the anisotropy depolarizes due to torsional motions about the long axis of a flexible filament, the anisotropy decays according to a more complex function (Allison & Schurr, 1979; Yoshimura et al., 1984):

$$r(t) = r_0\{\alpha_1 \exp[-(t/\Phi)^{1/2}] + \alpha_2 \exp[-(t/16\Phi)^{1/2}] + \alpha_3\} \quad (3)$$

Table 1: Steady-State Fluorescence Emission Anisotropy ($\bar{r}_f$) and Phosphorescence Emission Anisotropy ($\bar{r}_p$), and Phosphorescence Emission Lifetime (τ_p) of ErActin[a]

sample[b]	$\bar{r}_f$	$\bar{r}_p$	$\langle\tau_p\rangle$ (μs)
F-actin	0.361 ± 0.008	0.090 ± 0.005	275 ± 1
actoS1	0.358 ± 0.006	0.138 ± 0.006	373 ± 4
actoS1/ATP	0.365 ± 0.003	0.050 ± 0.005	288 ± 2
actoS1/ADP	0.352 ± 0.004	0.125 ± 0.002	330 ± 3
actoS1/ADP/P_i	0.353 ± 0.005	0.126 ± 0.003	333 ± 3

[a] ErActin is erythrosin-labeled actin. All measurements were done at 20 °C. The errors are standard deviations calculated from three or more measurements. [b] ActoS1 is a 1:1 complex; actoS1/ATP contained 20 mM ATP undergoing active ATP hydrolysis; actoS1/ADP/P_i contained ADP and P_i added at 20 mM; actoS1/ADP contained ADP added at 20 mM.

The r_0 and α_i terms have the same meaning and values as for eq 1, and Φ, the characteristic time for torsional twisting (Yoshimura et al., 1984), is directly proportional to the torsional rigidity of the filament.

The steady-state anisotropy corresponding to such a depolarization mechanism (assuming a single lifetime τ) is (Ludescher & Ludescher, 1993)

$$\bar{r}_{tor} = r_0\{\alpha_1 f(\tau/\Phi) + \alpha_2 f(\tau/16\Phi) + \alpha_3\} \quad (4)$$

where

$$f(\tau/\Phi) = 1 - (\pi\tau/4\Phi)^{1/2} \exp(\tau/4\Phi)\{1 - \mathrm{erf}[(\tau/4\Phi)^{1/2}]\} \quad (5)$$

and $f(\tau/16\Phi)$ is generated by replacing Φ with 16Φ in eq 4 and 5. Erf(z) is the error function of z.

Examination of eq 2 and 4 indicates that the steady-state anisotropy is sensitive to four molecular parameters; three of these, the initial anisotropy (r_0), the probe lifetime (τ), and the probe orientation on the surface of the filament (α_i), are properties of the spectroscopic probe; the fourth, the characteristic time for rotation (ϕ or Φ), is the only parameter that directly reflects the rotational dynamics of the filament. For all filament conditions studied in this report, we have performed control experiments to determine the relative changes in r_0, τ, or α_i; in the absence of such changes, we conclude that the change in anisotropy reflects a change in the rotational dynamic parameter (ϕ or Φ).

RESULTS

ActoS1 Dynamics in the Rigor Complex. The steady-state phosphorescence emission anisotropy ($\bar{r}_p$) of actin filaments labeled with erythrosin-5-iodoacetamide (ErActin) was 0.090 at 20 °C in F-buffer (Table 1). This value represents a time-averaged measurement of the rotational motions that occur during the excited triplet state lifetime of the probe. The erythrosin probe was shown in a previous study to be rigidly bound to the surface of F-actin (Ludescher & Liu, 1993), probably located near the monomer–monomer interface near the C-terminal of actin (Holmes et al., 1990). The average probe lifetime was 275 μs in F-actin (Table 1); the motions detected by this probe must thus have occurred on the microsecond time scale. We have shown (Ludescher & Liu, 1993) that the steady-state anisotropy of ErActin is sensitive to the binding of physiological ligands to the filaments; the anisotropy increased to 0.11 upon binding either the fungal toxin phalloidin, which stabilizes F-actin, or the regulatory protein tropomyosin. We therefore used the anisotropy to probe the interaction of myosin heads with F-actin.

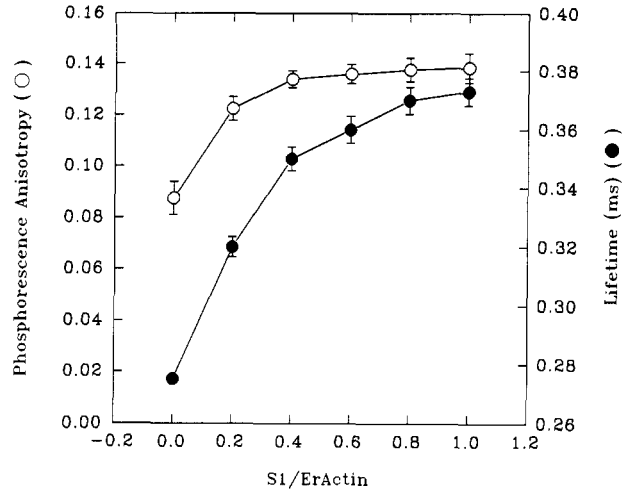

FIGURE 1: Phosphorescence emission lifetime and steady-state phosphorescence emission anisotropy of erythrosin-labeled F-actin as a function of the ratio of S1/actin in F-buffer at 20 °C.

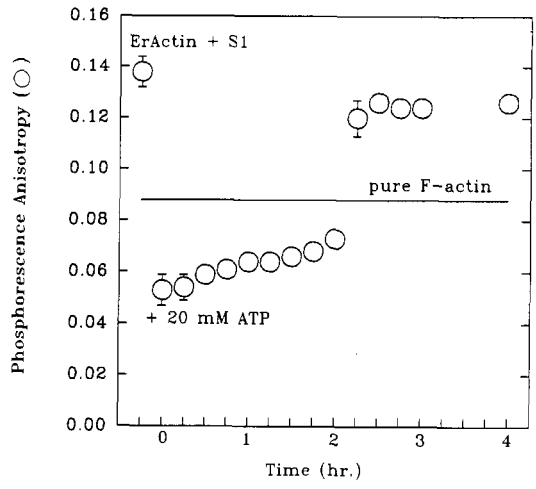

FIGURE 2: Steady-state phosphorescence emission anisotropy of erythrosin-labeled F-actin in a 1:1 complex with S1 measured as a function of time after the addition of 20 mM ATP in F-buffer at 20 °C.

Titration of ErActin filaments with isolated myosin heads, S1 fragments isolated by proteolysis with α-chymotrypsin, increased the steady-state anisotropy to 0.138 ± 0.006 at a 1:1 molar ratio of S1 to actin (Table 1 and Figure 1). The dynamic effects of S1 binding were not linear with the molar ratio of S1 to actin; $\bar{r}_p$ reaches a limiting high value at a stoichiometry of ≈0.4 S1/actin. The maximum value of the anisotropy at full saturation was only slightly less than 0.15, the value found for ErActin filaments immobilized on the microsecond time scale (Ludescher & Liu, 1993). Since the increase was nonlinear with the S1:actin ratio, the dynamic effect of S1 binding could reflect cooperative changes in F-actin structure (Prochniewicz et al., 1993).

A number of control experiments were done to establish that the increase in phosphorescence anisotropy was due to changes in the rotational dynamics of the filaments *per se* rather than due to trivial changes in probe properties. Measurements of the total phosphorescence intensity decays were used to estimate the average lifetime of the probe at each S1:actin ratio; the average lifetimes ($\langle\tau_p\rangle$) are also plotted versus S1:actin ratio in Figure 1. The probe lifetime increased from 275 ± 1 μs in F-actin to 373 ± 4 μs in the 1:1 actoS1 complex (Figure 1, Table 1); in contrast to the anisotropy titration, however, the average lifetime did not reach its maximum value at less than a 1:1 molar ratio of S1/actin. Such an increase in probe lifetime can only lead to a decrease in the measured steady-state anisotropy (see eq 2 and 4 under Materials and Methods).

The steady-state fluorescence emission anisotropy ($\bar{r}_f$), which is sensitive to fast motions of the erythrosin probe on the surface of actin (Ludescher & Liu, 1993), was also measured. The anisotropy values, 0.361 ± 0.008 for F-actin and 0.358 ± 0.006 for actoS1 (Table 1), were equal within experimental error, suggesting that S1 binding did not significantly change the independent motions of the probe on the surface of F-actin and thus did not increase r_0; the increase in phosphorescence anisotropy was thus not due to a trivial effect of S1 binding on the local motions of the probe. Measurements of the orientation of the probe absorption/fluorescence emission dipole on the filament, determined from studies of F-actin oriented by flow (Ng & Ludescher, 1994), have indicated that S1 binding did change the angle that this dipole makes with respect to the long axis of the filament and thus probably had no effect on the orientation of the phosphorescence emission dipole (α_i terms in eq 2 and 4); since the measured anisotropy of a filament is remarkably sensitive to the probe orientation with respect to the long filament axis (see Materials and Methods), these results indicated that the measured change in $\bar{r}_p$ was not a consequence of changes in probe orientation.

Steady-state phosphorescence anisotropy measurements thus suggest that the binding of myosin heads (S1) to F-actin nearly immobilized the rotational motions of the filaments on the microsecond time scale.

ActoS1 Dynamics during ATP Hydrolysis. The addition of ATP to the actoS1 complex induced a dramatic decrease in the steady-state phosphorescence emission anisotropy of actin filaments (Figure 2). Immediately after the addition of 20 mM MgATP to a solution of actoS1 at a 1:1 molar ratio, the phosphorescence emission anisotropy decreased from 0.138 to 0.050 ± 0.005, a value significantly lower than the anisotropy of pure actin filaments ($\bar{r}_p$ = 0.090). In the presence of 20 mM MgATP, the anisotropy increased after ≈2 h to 0.126 ± 0.002, a value slightly less than that seen in the actoS1 complex in the absence of nucleotide (Table 1 and Figure 2). In the presence of lower concentrations of MgATP, the increase in anisotropy occurred in shorter times (data not shown), suggesting that the increase was due to the depletion of available ATP in the solution. Under our experimental conditions, the MgATPase activity of actoS1 was 0.135 μmol of P_i (mg of S1)$^{-1}$ min^{-1}. At an S1 concentration of 1.3 mg/mL, the time needed to hydrolyze 20 mM MgATP was 114 min, approximately equal to the time observed (Figure 2) for the anisotropy to increase to the limiting high value. The new limiting anisotropy value (0.126) appeared to reflect the influence of ADP and P_i on the actoS1 interaction since the anisotropy of the actoS1/ADP/P_i complex prepared by direct addition of 20 mM ADP and 20 mM P_i to a 1:1 actoS1 complex was equal within experimental error to this value (Table 1).

The average lifetime of the probe in the actoS1 complex during ATP hydrolysis, 288 ± 2 μs (Table 1), was significantly smaller than the lifetime in the actoS1 complex without nucleotide but only marginally larger than the lifetime in pure F-actin. Since the presence of ATP actually decreased the average lifetime, whereas the measured decrease in the anisotropy would require an increase in lifetime, the decrease in anisotropy was not due to a trivial effect of the nucleotide on the probe lifetime. The fluorescence emission anisotropy

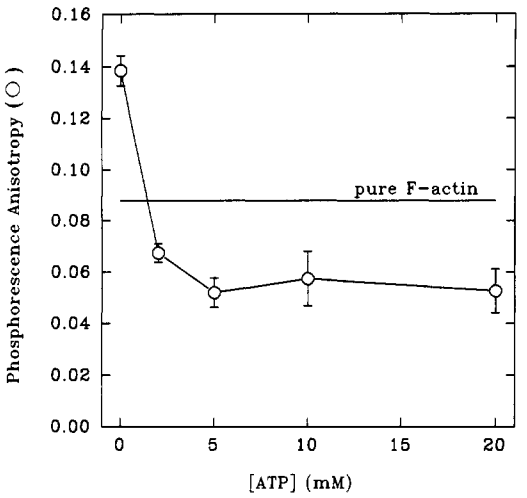

FIGURE 3: Steady-state phosphorescence emission anisotropy of a 1:1 complex of erythrosin-labeled F-actin with S1 measured as a function of ATP concentration in F-buffer at 20 °C.

of the probe also remained high during ATP hydrolysis (Table 1), suggesting that ATP hydrolysis did not decrease $\bar{r}_p$ by increasing the fast motions of the probe on the filament surface, and measurements of the probe orientation in oriented filaments indicated that ATP hydrolysis did not change the orientation of the probe on the filament surface (Ng & Ludescher, 1994).

Active ATP hydrolysis by myosin heads within the actoS1 complex thus appeared to induce rotational motions of or within the actoS1 filament.

Influence of Nucleotide Concentration on F-Actin Dynamics. The effect of ATP concentration on the phosphorescence anisotropy of the actoS1 complex is shown in Figure 3. The anisotropy decreased as the ATP concentration increased and leveled off at a value of about 0.050 at high [ATP]. Due to the limitations of our instrument, a single anisotropy measurement required 15 min of signal-averaging; the measurement thus represents the anisotropy of the sample averaged over this 15 min interval. If the time needed to deplete the available ATP in the solution was less than 15 min, then the measured anisotropy would appear too high due to significant averaging of the motion of the actoS1/ADP/P_i state. Under our experimental conditions, it took only 11 min for actoS1 to hydrolyze a 2 mM MgATP solution to ADP and P_i. Thus, the anisotropy measured at 2 mM ATP, $\bar{r}_p$ = 0.066, was probably an overestimate of the actual anisotropy at this nucleotide concentration; the phosphorescence anisotropy of actoS1 was thus essentially independent of ATP concentration over the range from about 2 to 20 mM. Control experiments indicated that the anisotropy of actoS1 in F-buffer was not affected by ionic strength over the range from 100 to 300 mM KCl and that the anisotropy of pure F-actin (without S1) was not modulated by ATP over the concentration range from 0.2 to 20 mM.

The anisotropy of the state generated by adding ADP at a concentration of 20 mM directly to a 1:1 complex of actoS1 was identical in magnitude, 0.125 ± 0.002, to that generated by the addition of both ADP and P_i (0.126 ± 0.003). The environment of the probe in both of these states was also similar since the measured fluorescence anisotropies and phosphorescence lifetimes were identical within experimental error (Table 1) and the probe orientations in these two states were the same as that seen in the actoS1 or actoS1/ATP states (Ng & Ludescher, 1994).

DISCUSSION

F-Actin has a high steady-state phosphorescence anisotropy (0.138) in a rigor complex with S1, an intermediate anisotropy (0.090) in pure filaments, and a low anisotropy (0.050) during ATP hydrolysis in the presence of S1. These data provide strong evidence that ATP hydrolysis on myosin heads bound to F-actin induces large-scale rotational motions in the filaments on the microsecond time scale. We will discuss here the credibility of this conclusion, outline possible physical interpretations of the results, and relate these interpretations to previous data on the role that F-actin plays during force generation.

Steady-State Anisotropy and the Rotational Dynamics of F-Actin. The emission anisotropy can provide a direct measurement of the rotational motion of a chromophore during its excited state lifetime; as with any technique involving molecular probes, however, the results must be interpreted with caution. Certain physical and photophysical properties of the probe *per se* can obscure the direct connection between the measured anisotropy and the rotational motion of the protein complex to which the probe is attached (Ludescher et al., 1987). This caveat especially applies to steady-state measurements of the anisotropy because they reflect an average of all possible modes of reorientation of the emission dipole that occur during, in our case, the excited triplet state lifetime of the erythrosin probe. The primary problem is to ensure that the measured changes in anisotropy actually reflect changes in the large-scale rotational dynamics of F-actin and not changes in the properties of the erythrosin probe.

There are three primary properties of the probe that can influence the steady-state phosphorescence anisotropy of F-actin (see Materials and Methods, especially eq 2 and 4): local motions of the probe on the filament surface that modulate r_0, the probe triplet lifetime (τ), and the orientation of the probe with respect to the filament axis that determines α_l. Changes in any one of these properties can change the measured anisotropy without a corresponding change in the dynamics of the filament.

Rapid motions of the probe can directly influence the steady-state anisotropy by modulating r_0; since the steady-state measurement cannot distinguish between the rates of the detected motions, fast motions of the probe and slow motions of the filament are indistinguishable as long as they occur within the excited state lifetime. We have estimated the local motions of the probe through measurements of the steady-state fluorescence anisotropy which provides an average measure of probe motions during the excited singlet lifetime. Unfortunately, this measurement provides an underestimate of probe motions because of the short erythrosin singlet lifetime of several hundred picoseconds (Jovin et al., 1981). Although we found no significant changes in the probe fluorescence anisotropy during interaction with myosin heads in the presence and absence of nucleotides, suggesting that these interactions did not perturb r_0, it is possible that there were changes in slower probe motions that were undetected by the fluorescence measurement. However, time-resolved anisotropy measurements of the rotational motions of the surface-exposed tryptophan side chain of phospholipase A_2, for example, indicate that this aromatic chromophore undergoes limited independent motion on the hundreds of picoseconds time scale (Ludescher et al., 1988; Jain & Maliwal, 1993), and a recent X-ray crystallography study of the aromatic chromophore 1,5-IAENS covalently bound to ribonuclease A indicates that this aromatic probe is rigidly attached through noncovalent interactions with the protein surface (Baudet-Nessler et al.,

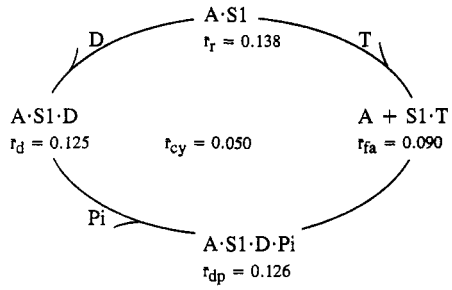

FIGURE 4: Simplified schematic of the actoS1 ATPase cycle; A is actin, S1 is myosin subfragment 1, T is ATP, D is ADP, and P_i is inorganic phosphate. The measured value of the steady-state anisotropy of erythrosin-labeled F-actin in each intermediate state is listed under that state. See text for details.

1993). The possibility of probe motions in the nanosecond range is thus unlikely.

Regardless of the motional model used to describe F-actin depolarization (outlined under Materials and Methods), the steady-state anisotropy is related to the ratio of the excited state lifetime (τ) to the characteristic time for the rotational motion (ϕ or Φ): an increase in this ratio decreases the anisotropy, and vice versa, irrespective of whether this change is due to a change in τ or to a change in ϕ or Φ. Our measurements of the average lifetime of the probe under each set of conditions demonstrated that the changes in anisotropy cannot be explained away as the result of changes in the probe lifetime; in each case, the anisotropy changed in a direction opposite to that expected from a change in the lifetime.

In addition, finally, the phosphorescence anisotropy, either steady-state or time-resolved, is sensitive to the orientation of the probe on the surface of the filament (Brand et al., 1985; Yoshimura et al., 1984). For the long, asymmetric actin filament, motions on the microsecond time scale primarily reflect rotations about the long axis of the filament; as outlined under Materials and Methods, these motions may be due either to rigid body rotations or to internal torsional twisting motions. Regardless of the physical origin of the motions, however, the influence of such rotations on the anisotropy is directly related to the orientation of the probe emission dipole with respect to the long axis (α_i). Since any change in this orientation can have a large effect on the anisotropy, we measured the orientation of the absorption/fluorescence dipole of erythrosin on the F-actin surface (Ng & Ludescher, 1994); this angle, 42°, was unaffected by S1 binding or the presence of nucleotides. Although it is possible that the phosphorescence emission dipole, but not the absorption/fluorescence dipole, was affected by these conditions and that this perturbation caused a change in the phosphorescence anisotropy, this possibility is remote because of the fixed angular relationship between the absorption and phosphorescence emission dipoles.

We thus conclude that the changes in steady-state phosphorescence anisotropy measured in this study reflected real changes in the molecular dynamics of the actoS1 filament and not trivial changes in the properties of the erythrosin probe.

Physical Interpretations of the Anisotropy Measurements. A simplified schematic of the ATPase cycle in actoS1 is shown in Figure 4. Four intermediate states are indicated, and the apparent phosphorescence anisotropy for each state is listed. The A·S1, or rigor, state was generated in the cuvette and the anisotropy measured directly, while the A + S1·T state was modeled by free F-actin; the other two states, A·S1·D·P_i and A·S1·D, in which the ATP hydrolysis products are present in the actoS1 complex, were modeled by addition of exogenous ADP + P_i or ADP to actoS1. The anisotropy for the ensemble of states in which actoS1 is actively hydrolyzing ATP and thus populating the various states in the cycle is $\bar{r}_{cy}$.

There are two alternate interpretations for the low value of the anisotropy seen during ATP hydrolysis; we will call these two interpretations the flexible state and the induced motion models. In the flexible state model, the influence of ATP hydrolysis on the actoS1 dynamics is due to the presence of an intermediate state in the cycle with a low anisotropy; this intermediate state must be in a conformation that is significantly more flexible than pure F-actin so that the population of this intermediate during the ATPase cycle would decrease the anisotropy. In the context of this model, the anisotropy of some intermediate state(s), for example, $\bar{r}_{dp}$ or $\bar{r}_d$, must be very low in order to account for the low value of $\bar{r}_{cy}$. However, the measured anisotropy of the A·S1·D·P_i state, 0.126 (Table 1), is significantly higher than the value for pure E-actin ($\bar{r}_{fa}$ = 0.09), suggesting that the filament in this state of the cycle is actually more rigid than pure F-actin and that population of this state cannot account for the low value of the anisotropy during ATP hydrolysis. The same argument also applies to the A·S1·D state since the anisotropy of actoS1/ADP is also 0.125 (Table 1). We thus conclude that the flexible state model cannot satisfactorily explain our results.

In the induced motion model, the decrease in the anisotropy reflects some additional rotational motion of the actoS1 filament that is induced during the ATPase cycle. This motion could be induced during the transition from one state of the ATPase cycle to another, as, for example, during the transition from A·S1·ADP·P_i to A·S1·ADP involving release of phosphate. The motions could reflect novel modes of motion of the actoS1 filament peculiar to the force generation process, or they could reflect an activation or enhancement of the usual modes of motion of the actin filament. It is also possible, however, that the anisotropy reflects internal mobility within the attached S1 rather than within the actin filament.

The erythrosin lifetime data (Figure 1 and Table 1) suggest that S1 binding changes the local environment of the probe, perhaps through a direct interaction; if so, however, this interaction does not change either the probe orientation (Ng & Ludescher, 1994) or the local probe motion(s) on the surface of the filament (Table 1). Direct interaction between S1 and the probe during the ATPase cycle raises the possibility that the observed decrease in anisotropy reflects internal mobility within attached myosin heads (S1) rather than within F-actin.

Our studies of the probe dipole orientation on the actin filament provide constraints on the possible induced motions during force generation since the erythrosin fluorescence dipole orientation on F-actin is unaffected by S1 binding or by the presence of the nucleotides ATP, ADP, or ADP + P_i (Ng & Ludescher, 1994). These data imply that the induced motion(s) do(es) not change the probe orientation with respect to the long filament axis. Rotations, either local or global, about the long axis of the filament are the only motions that satisfy such a constraint.

An additional constraint is provided by the requirement that the motions occur within the excited states lifetime of the probe (288 μs during ATP hydrolysis). The actoS1 turnover rate was 0.23 s^{-1} under our experimental conditions [based on an ATPase activity of 0.135 μmol of P_i (mg of S1)$^{-1}$ min^{-1}]; at a molar ratio of 1 S1/actin, each actin monomer participated with S1 in an ATP hydrolysis event approximately once every 4.4 s. We can make a rough calculation of the fraction of this cycle time that an erythrosin molecule was in the excited triplet state and thus capable of detecting any induced rotational

motion. The probes were excited by a pulsed lamp operating at 30 Hz; since the lamp pulse was narrow (FWHM of less than 10 μs), each probe could be excited to the triplet state only once per pulse. During the 4.4 s required for each ATP hydrolysis event, the lamp flashed 132 times, and, assuming that each lamp flash excited every erythrosin probe (an upper limit on the number of excited probes), the labeled actin molecules spent $\approx$0.04 s (132 times the excited state lifetime of 3×10^{-4} s) in the excited state. Thus, during each ATP hydrolysis event, the erythrosin probes were in the triplet state, and thus in a position to report on filament rotational motion, only about 1% of the time (0.04/4.4).

Since the hydrolysis events were not synchronous with probe excitation, the detection of appreciable rotational motion during such a short observation window suggests that ATP hydrolysis increased the global rather than the local rotational motions of the actoS1 filament. If the induced motions were localized in time and space, corresponding to the local rotation of a single actin monomer, for example, or to internal mobility within attached myosin heads detected through direct interaction between S1 and the erythrosin probe, they would not be detected during the small sampling time by a large enough fraction of the probes to cause the observed decrease in the anisotropy. We therefore conclude that the motions induced during ATP hydrolysis involve large-scale fluctuations of the entire filament occurring on the microsecond time scale.

Relation to Previous Data on the Dynamics of F-Actin during Force Generation. Recent descriptions of the behavior of F-actin in *in vitro* motility assays indicate that myosin induces right-handed twisting motions about the long axis of F-actin (Tanaka et al., 1992; Nishizaka et al., 1993). Previous spectroscopic studies have also suggested that the rotational motion of F-actin on the microsecond time scale is due to the twisting of a long filament with internal torsional flexibility (Yoshimura et al., 1984); recent time-resolved phosphorescence anisotropy measurements have provided additional evidence that the primary rotational motions of F-actin involve long axis torsional twisting motions (Prochniewicz et al., 1994; Zhang et al., 1994). We speculate that the phosphorescence anisotropy provides a direct measurement on the microsecond time scale of the same long axis twisting motions seen in actomyosin in the *in vitro* motility assay; in our measurements, however, the induced twisting motions were generated in isotropic solution by myosin heads. Whether these motions are unique to the force-generating event or whether they reflect an activation of the normal torsional modes of the filament is unclear from our data.

These steady-state measurements provide tantalizing indications that large-scale torsional motions within the actin filament are essential components of the force-generating event in actomyosin contraction. However, this study provides no direct evidence on the precise physical nature of these motions. Such evidence will come from detailed time-resolved studies of the rotational motion of F-actin in isotropic solution and in ordered arrays using phosphorescence anisotropy from triplet probes attached to Cys374 and other sites and the effect of physiological and physical perturbations on these motions. These studies are underway.

REFERENCES

Allison, S., & Schurr, M. (1979) *Chem. Phys. 41*, 35.

Bagshaw, C. (1982) *Muscle Contraction*, Chapman and Hall, New York.

Baudet-Nessler, S., Jullien, M., Crosio, M. P., & Janin, J. (1993) *Biochemistry 32*, 8457.

Brand, L., Knutson, J. R., Davenport, L., Beechem, J. M., Dale, R. E., Walbridge, D. G., & Kowalczyk, A. A. (1985) in *Spectroscopy and the Dynamics of Molecular Biological Systems* (Bayley, P. M., & Dale, R. E., Eds.) pp 259–319, Academic Press, London.

Burlacu, S., & Borejdo, J. (1992) *Biophys. J. 63*, 1471.

Cherry, R. J. (1985) in *Spectroscopy and the Dynamics of Molecular Biological Systems* (Bayley, P. M., & Dale, R. E., Eds.) pp 79–93, Academic Press, London.

Drummond, D. R., Peckham, M., Sparrow, J. C., & White, D. C. S. (1990) *Nature 348*, 440.

Eads, T. M., Thomas, D. D., & Austin, R. H. (1984) *J. Mol. Biol. 178*, 55.

Holmes, K. C., Popp, D., Gebhard, W., & Kabsch, W. (1990) *Nature 347*, 44.

Horie, T., & Vanderkooi, J. M. (1981) *Biochim. Biophys. Acta 670*, 294.

Jain, M. K., & Maliwal, B. P. (1993) *Biochemistry 32*, 11838.

Jovin, T., Bartholdi, M., Vaz, W. L. C., & Austin, R. H. (1981) *Ann. N.Y. Acad. Sci. 366*, 176.

Kabsch, W., Mannherz, H. G., Suck, D., Pai, E. F., & Holmes, K. C. (1990) *Nature 347*, 37.

Ludescher, R. D., & Liu, Z. (1993) *Photochem. Photobiol. 58*, 858.

Ludescher, R. D., & Ludescher, W. H. (1993) *Photochem. Photobiol. 58*, 881.

Ludescher, R. D., Peting, L., Hudson, S., & Hudson, B. (1987) *Biophys. Chem. 28*, 59.

Ludescher, R. D., Johnson, I. D., Volwerk, J. J., de Haas, G. H., Jost, P. C., & Hudson, B. S. (1988) *Biochemistry 27*, 6618.

Menetret, J. F., Hofman, W., Schroder, R. R., Rapp, G., & Goody, R. S. (1991) *J. Mol. Biol. 219*, 139.

Morel, J., & Merah, Z. (1992) *J. Muscle Res. Cell Motil. 13*, 5.

Ng, C. M., & Ludescher, R. D. (1994) *Proc. SPIE—Int. Soc. Opt. Eng.* (in press).

Nishizaka, T., Yagi, T., Tanaka, Y., & Ishiwata, S. (1993) *Nature 361*, 269.

Pardee, J. D., & Spudich, J. A. (1982) *Methods Enzymol. 85B*, 164.

Prochniewicz, E., & Yanagida, T. (1990) *J. Mol. Biol. 216*, 761.

Prochniewicz, E., Katayama, E., Yanagida, T., & Thomas, D. D. (1993) *Biophys. J. 65*, 113.

Prochniewicz, E., Zhang, Q., & Thomas, D. D. (1994) *Biophys. J. 66*, A194.

Rayment, I., Rypniewski, W. R., Schmidt-Base, K., Smith, R., Tomchick, D. R., Benning, M. M., Winkelmann, D. A., Wesenberg, G., & Holden, H. M. (1993a) *Science 261*, 50.

Rayment, I., Holden, H. M., Whittaker, M., Yohn, C. B., Lorenz, M., Holmes, K. C., & Milligan, R. A. (1993b) *Science 261*, 58.

Sawyer, W. H., Woodhouse, A. G., Czarnecki, J. J., & Blatt, E. (1988) *Biochemistry 27*, 7733.

Schwyter, D. H., Kron, S. J., Toyoshima, Y. Y., Spucich, J. A., & Reisler, E. (1990) *J. Cell. Biol. 111*, 465.

Tanaka, Y., Ishijima, A., & Ishiwata, S. (1992) *Biochim. Biophys. Acta 1159*, 94.

Thomas, D. D., Seidel, J. C., & Gergely, J. (1979) *J. Mol. Biol. 132*, 257.

Thomas, D. D., Ishiwata, S., Seidel, J. C., & Gergely, J. (1980) *Biophys. J. 32*, 873.

Wahl, P., Meyer, G., Parrod, J., & Auchet, J.-C. (1970) *Eur. Polym. J. 6*, 585.

Weeds, A. G., & Taylor, R. S. (1975) *Nature 257*, 54.

Yanagida, T., Nakase, M., Nishiyama, K., & Oosawa, F. (1984) *Nature 307*, 58.

Yoshimura, H., Nishio, T., Mihashi, K., Kinosita, K., & Ikegami, A. (1984) *J. Mol. Biol. 179*, 453.

Zhang, Q., Prochniewicz, E., & Thomas, D. D. (1994) *Biophys. J. 66*, A390.